Electronic Supplementary Information

Determination of thallium(III) ions by oxidative hydrolysis of rhodamine-hydroxamate

Jae Hoon Yoo, Yu Jeong Lee, Kang Min Lee, Myung Gil Choi, Tae Jung Park,* and Suk-Kyu Chang*

Department of Chemistry, Chung-Ang University, Seoul 06974, Republic of Korea

Contents

Experimental details.

Preparation of Probes 1 and 2

Distilled water (20 mL) containing a solution of hydroxylamine hydrochloride (1.40 g, 20 mmol) and sodium hydroxide (0.80 g, 20 mmol) was added to an ethanol solution (20 mL) of rhodamine 6G (0.96 g, 2.0 mmol) or rhodamine B base (0.88 g, 2.0 mmol). After 2 hours of stirring at 25 °C, 200 mL of water was added. Dichloromethane was used to extract the product while anhydrous magnesium sulfate was used to dry the organic phase. A column chromatography made up of silica gel was used for the purification of the crude product (eluant: ethyl acetate).

Probe **1**.[S1] Light pink solid, 0.66 g, 77%. ^{1}H NMR (600 MHz, chloroform-*d*) δ 7.85 – 7.81 (m, 1H), 7.46 – 7.39 (m, 2H), 7.26 (s, 1H), 7.06 – 7.01 (m, 1H), 6.40 (s, 2H), 6.36 (s, 2H), 3.22 (q, J = 7.2 Hz, 4H), 1.91 (s, 6H), 1.32 (t, J = 7.1 Hz, 6H); ^{13}C NMR (150 MHz, $CDCl_3$) δ 163.52, 152.14, 150.82, 147.55, 132.63, 128.49, 128.08, 127.72, 123.60, 122.80, 117.75, 104.69, 96.99, 65.85, 38.36, 16.76, 14.77; MS (EI); *m/z* calculated for $C_{26}H_{27}N_3O_3$ $[M]^+$: 429.2, found 429.0.

Probe **2**.[S2] Light pink solid, 0.68 g, 75%. ^{1}H NMR (600 MHz, chloroform-*d*) δ 7.83 (d, J = 7.4 Hz, 1H), 7.42 (dt, J = 20.0, 7.3 Hz, 2H), 7.08 (d, J = 7.4 Hz, 1H), 6.52 (d, J = 8.8 Hz, 2H), 6.43 (d, J = 2.6 Hz, 2H), 6.29 (dd, J = 8.8, 2.6 Hz, 2H), 3.34 (q, J = 7.1 Hz, 8H), 1.17 (t, J = 7.0 Hz, 12H); ^{13}C (150 MHz, $CDCl_3$) δ 163.56, 153.76, 150.63, 148.94, 132.59, 128.71, 128.12, 128.03, 123.65, 122.86, 107.93, 104.22, 98.11, 65.82, 44.36, 12.62; MS (EI); *m/z* calculated for $C_{28}H_{32}N_3O_3$ $[M+H]^+$: 458.2, found 458.2.

Table S1. Summarization of reported Tl^{3+}-selective determination methods

Compound	Signal	Conditions	LOD[a]	Mechanism	Applications	Ref.
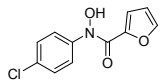	Colorimetry	pH 7.0 solution containing 0.1% $CHCl_3$	-	Formation of hydroxamic acid-Tl^{3+} complex	Tl^{3+} detection in standard samples	[S3]
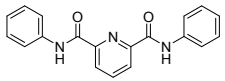	Colorimetry	pH 1.0 Glycine-HCl buffer	1.2×10^{-9} M (preconcentration)	Extraction of Tl^{3+} by 2,6-bis(*N*-phenyl carbamoyl) pyridine	Tl^{3+} detection in drinking water, river water, and human serum	[S4]
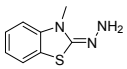	Colorimetry	H_2PO_4 medium	7.2×10^{-5} M	Oxidative coupling reaction of **MBTH** with **IDH**	Tl^{3+} detection in practical water samples and urine	[S5]
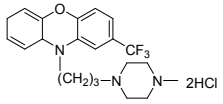	Colorimetry	H_2PO_4 medium	2.6×10^{-5} M	Oxidation of trifluoperazine-HCl	Tl^{3+} detection in alloys, minerals, and urine.	[S6]
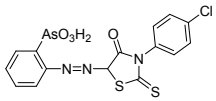	Fluorescence	Acetone containing 10% (*v*/*v*) HCl	1.3×10^{-12} M (preconcentration)	Oxidation of arsenoxylphenylazo rhodanine	Tl^{3+} detection in wine, water and mineral samples	[S7]
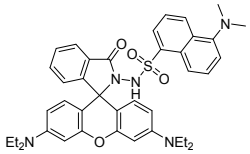	Colorimetry & Fluorescence	Acetate buffer (pH 4.76) with 20% (*v*/*v*) DMSO	1.9×10^{-7} M	Oxidative hydrolysis to rhodamine b base	Scanner-based Tl^{3+} determination of commercial reagent	[S8]

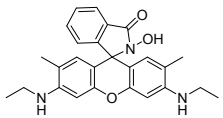	Colorimetry & Fluorescence	Acetate buffer (pH 4.2) comprising 30% (*v/v*) DMSO	2.9×10^{-7} M	Oxidative hydrolysis to rhodamine 6G	Determination of urinary Tl^{3+} ion using a smartphone-based method	This work

[a] Limit of detection.

References.

[S1] Y. K. Yang, H. J. Cho, J. Lee, I. Shin and J. Tae, *Org. Lett.*, 2009, **11**, 859–861.

[S2] T. Sun, J. O. Moon, M. G. Choi, Y. Cho, S. W. Ham and S.-K. Chang, *Sens. Actuator B-Chem.*, 2013, **182**, 755–760.

[S3] Y. K. Agrawal and V. J. Bhatt, *Analyst*, 1986, **111**, 761–765.

[S4] B. Rezaei, S. Meghdadi and N. Majidi, *Spectroc. Acta Pt. A-Molec. Biomolec. Spectr.*, 2007, **67**, 92–97.

[S5] P. Nagaraja, N. G. S. Al-Tayar, A. Shivakumar, A. K. Shresta and A. K. Gowda, *J. Mex. Chem. Soc.*, 2009, **53**, 201–208.

[S6] H. D. Revanasiddappa and T. N. K. Kumar, *Anal. Sci.*, 2002, **18**, 1131–1135.

[S7] S. Ge, P. Dai, J. Yu, Y. Zhu, J. Huang, C. Zhang, L. Ge and F. Wan, *Intern. J. Environ. Anal. Chem.*, 2010, **90**, 1139–1147.

[S8] Y. J. Lee, M. G. Choi, J. H. Yoo, T. J. Park, S. Ahn and S.-K. Chang, *J. Photochem. Photobiol. A-Chem.*, 2020, **394**, 112471.

(a)

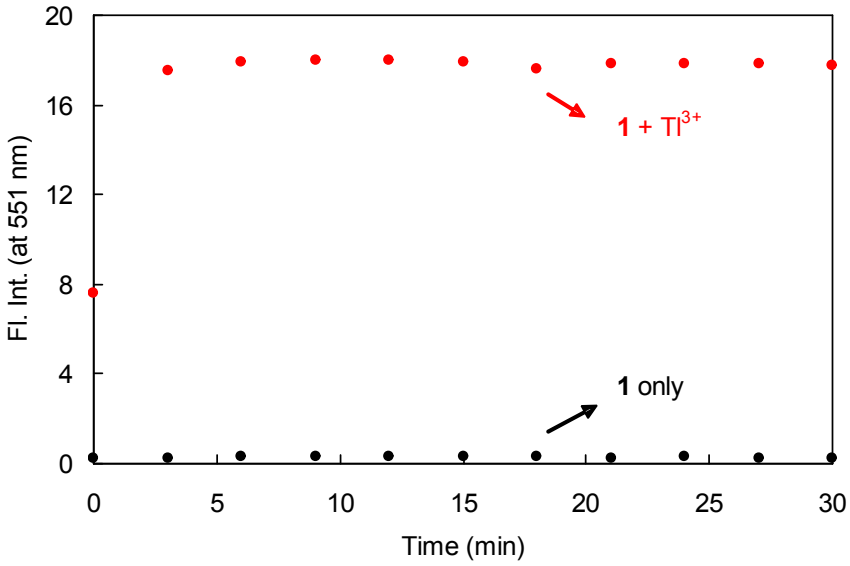

(b)

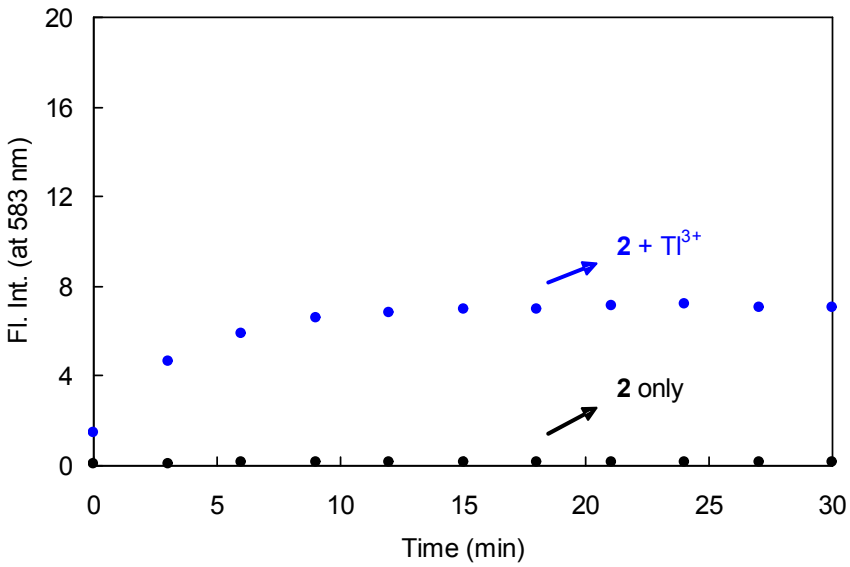

Fig. S1. Time plot of fluorescence Tl^{3+} signaling by probes (a) **1** and (b) **2** monitored at 551 nm (for probe **1**) and 583 nm (for probe **2**). [**1**] = [**2**] = 5.0×10^{-6} M, [Tl^{3+}] = 1.5×10^{-3} M in acetate buffer solution (pH 4.2, 10 mM) containing 30% (*v*/*v*) DMSO. λ_{ex} = 527 nm.

(a)

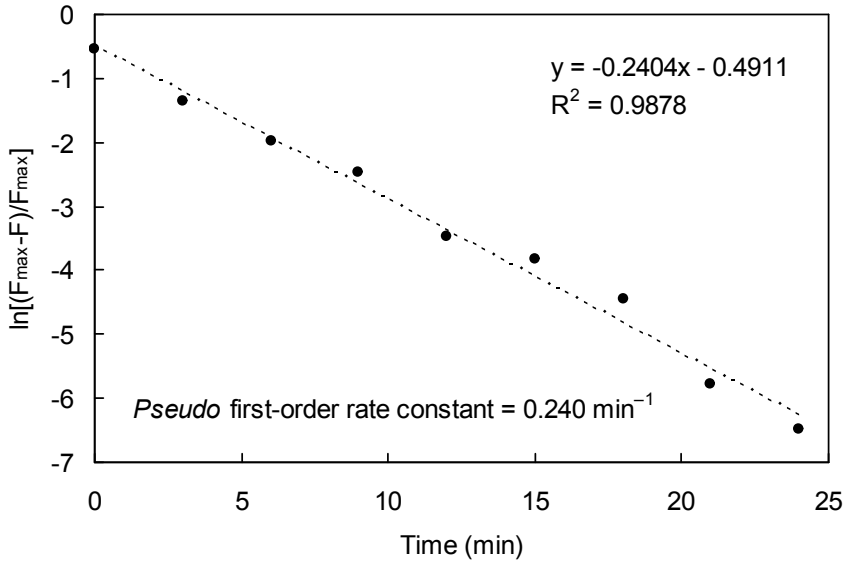

(b)

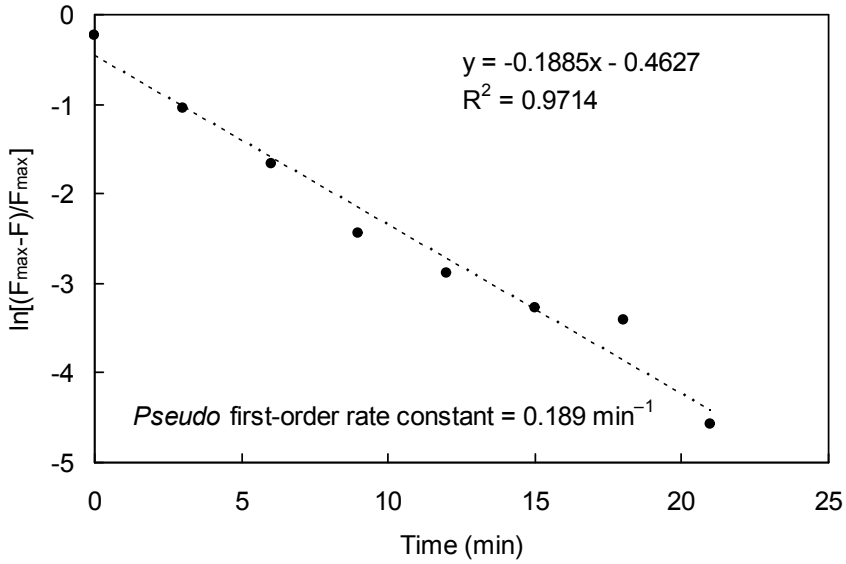

Fig. S2. *Pseudo*-first-order kinetic plot of the reaction of probes (a) **1** and (b) **2** with Tl^{3+}. [**1**] = [**2**] = 5.0×10^{-6} M, $[Tl^{3+}] = 1.5 \times 10^{-3}$ M in a solution of acetate buffer (pH 4.2, 10 mM) comprising 30% (*v/v*) DMSO. λ_{ex} = 527 nm.

(a)

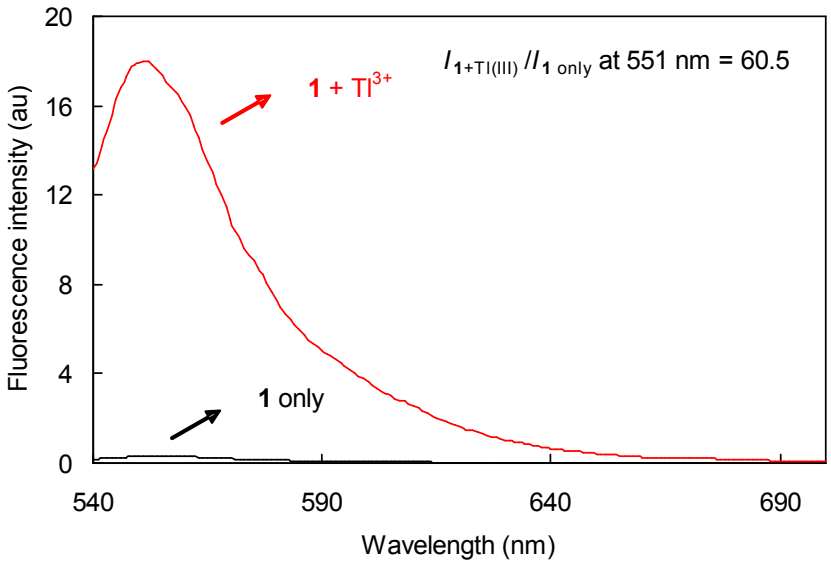

(b)

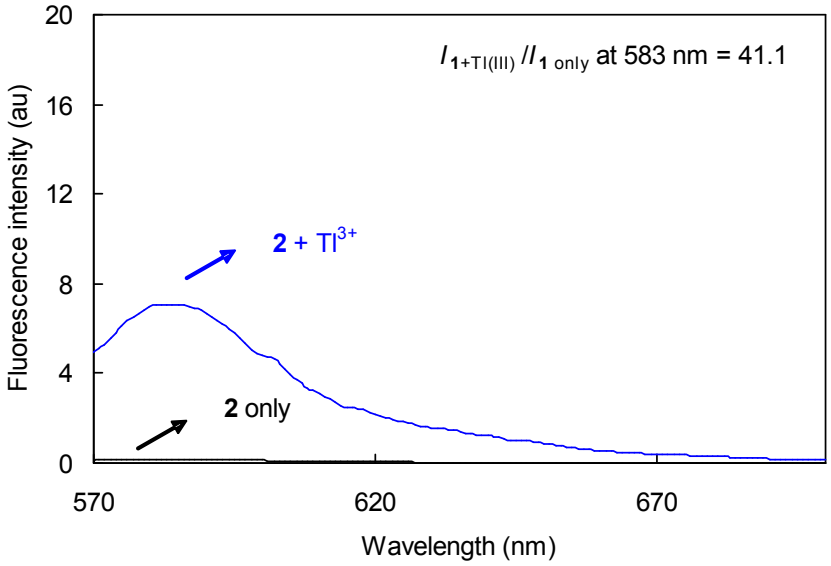

Fig. S3. Fluorescence spectra of (a) **1** and (b) **2** in the presence and absence of Tl^{3+} ions. [**1**] = [**2**] = 5.0×10^{-6} M, [Tl^{3+}] = 1.5×10^{-3} M in acetate buffer solution (pH 4.2, 10 mM) containing 30% (*v*/*v*) DMSO. λ_{ex} = 527 nm for probe **1** and 559 nm for probe **2**.

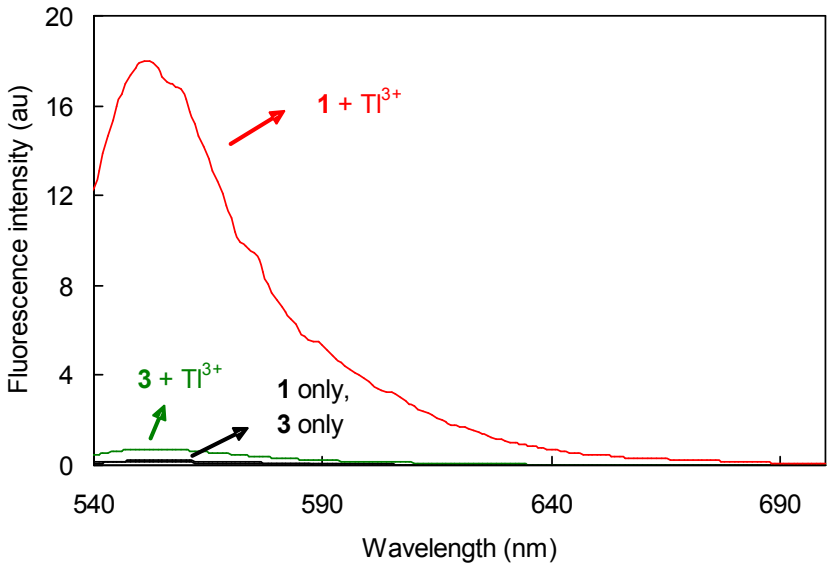

Fig. S4. Fluorescence spectra of **1** and **3** in the presence and absence of Tl^{3+} ions. [**1**] = [**3**] = 5.0×10^{-6} M, $[Tl^{3+}] = 1.5 \times 10^{-3}$ M in acetate buffer solution (pH 4.2, 10 mM) containing 30% (*v*/*v*) DMSO. λ_{ex} = 527 nm.

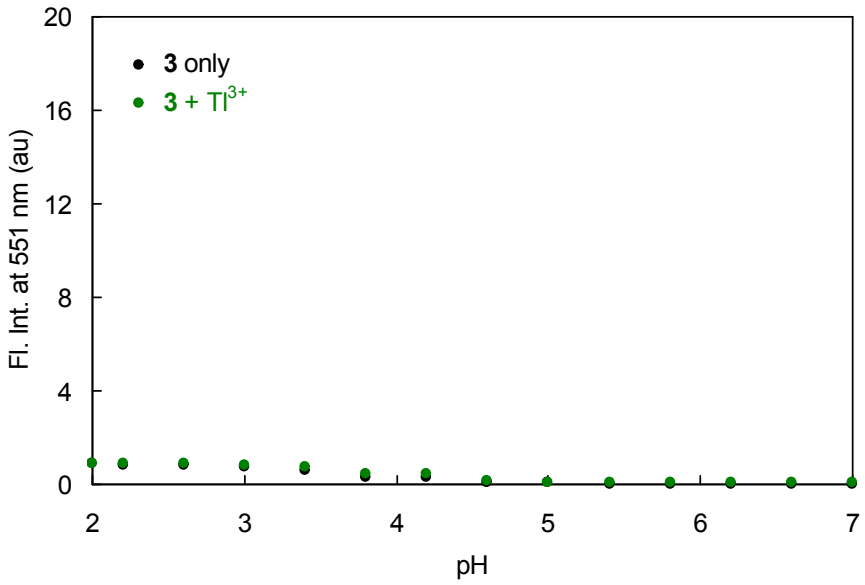

Fig. S5. Effect of pH on the fluorescence signaling of Tl^{3+} by compound **3**. [**3**] = 5.0×10^{-6} M, $[Tl^{3+}] = 1.5 \times 10^{-3}$ M in acetate buffer solution (pH 4.2, 10 mM) containing 30% (*v*/*v*) DMSO. pH of measuring solutions was adjusted using 0.1 N HCl and NaOH solutions. λ_{ex} = 527 nm.

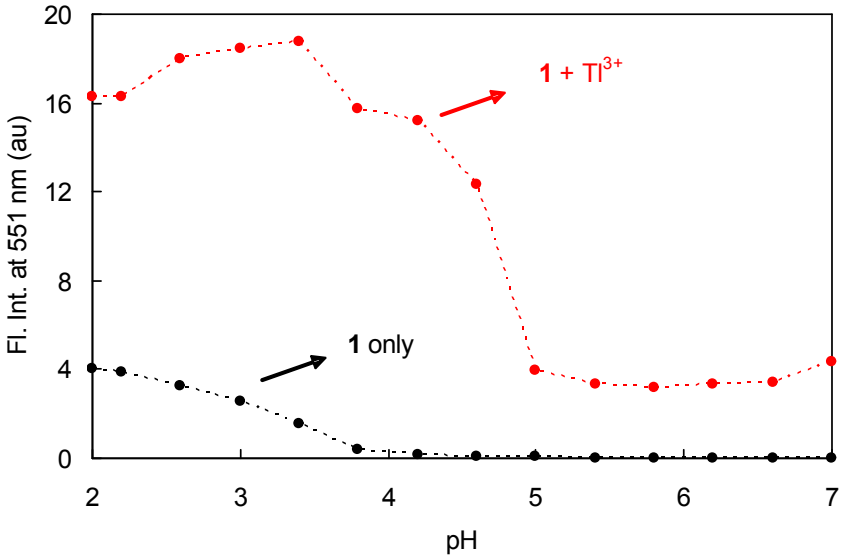

Fig. S6. Effect of pH on the fluorescence signaling of Tl^{3+} by probe **1**. Data for the alkaline (pH > 7.0) conditions were not obtained as described in the main text. [**1**] = 5.0×10^{-6} M, $[Tl^{3+}] = 1.5 \times 10^{-3}$ M in acetate buffer solution (pH 4.2, 10 mM) containing 30% (*v*/*v*) DMSO. pH of measuring solutions was adjusted using 0.1 N HCl and NaOH solutions. λ_{ex} = 527 nm.

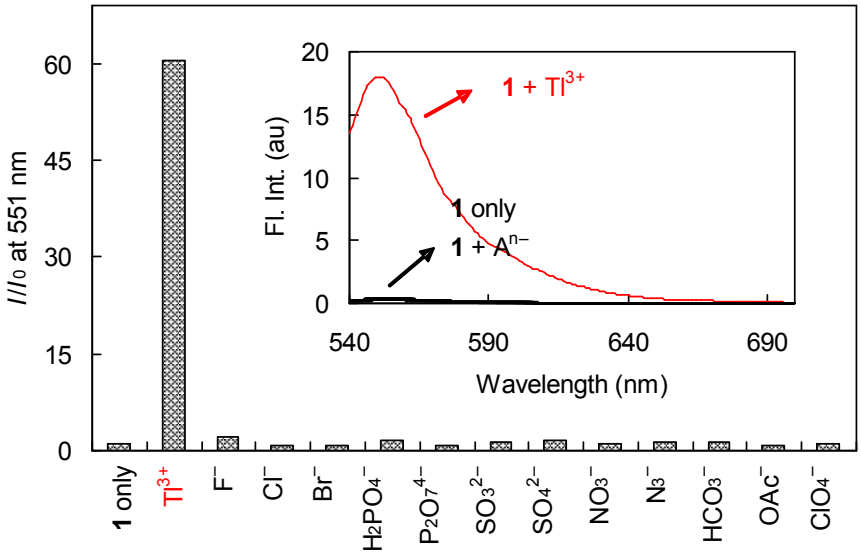

Fig. S7. Changes in fluorescence enhancement (I/I_0) of probe **1** at 551 nm in the presence of Tl^{3+} ions or common anions. Inset: fluorescence spectra of **1** in the presence of anions. [**1**] = 5.0×10^{-6} M, $[Tl^{3+}] = [A^{n-}] = 1.5 \times 10^{-3}$ M in acetate buffer solution (pH 4.2, 10 mM) containing 30% (*v*/*v*) DMSO. λ_{ex} = 527 nm.

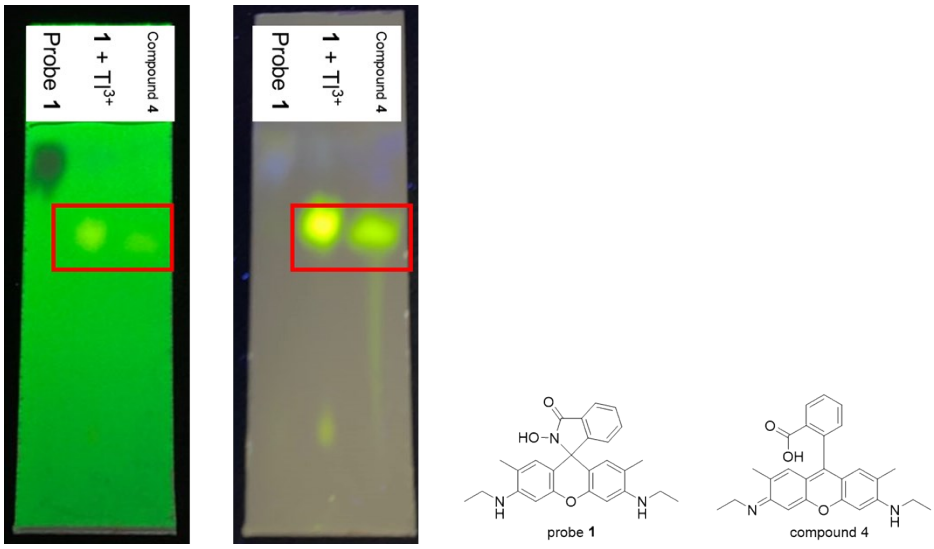

Fig. S8. Picture of TLC plate showing the migration of probe **1**, **1** in the presence of Tl^{3+}, and reference **4**. Silica gel TLC plate under illumination with 254 nm (left) and 365 nm (right) of light, eluent: CH_2Cl_2:CH_3OH = 9:1 (*v*/*v*).

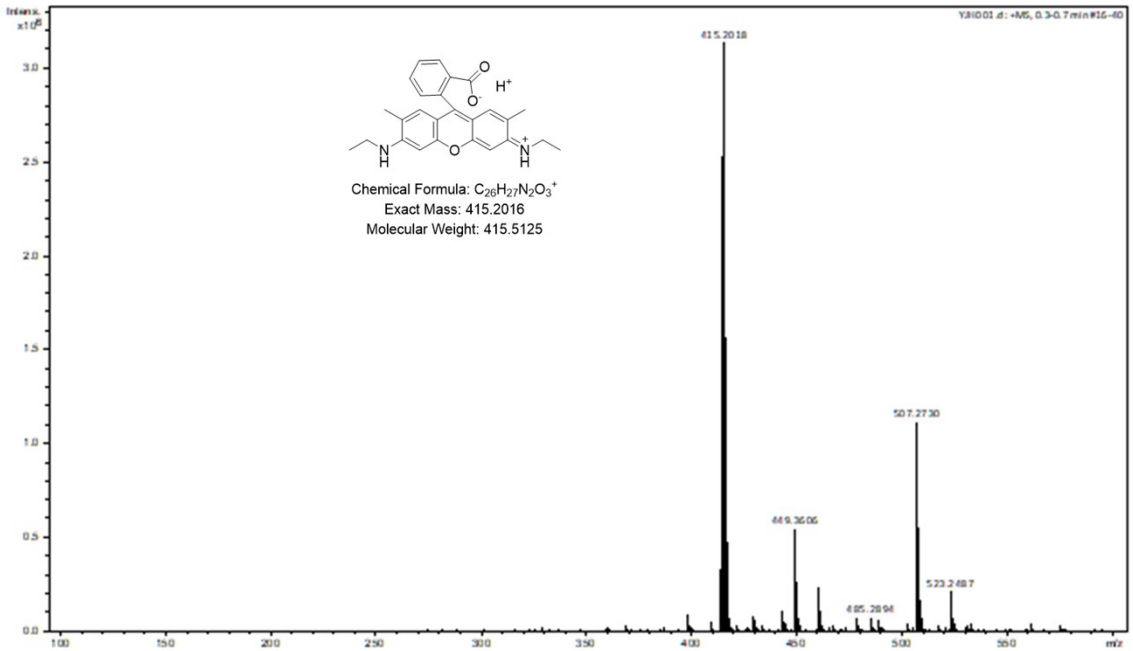

Fig. S9. Mass spectrum of Tl^{3+} signaling product of **1**.

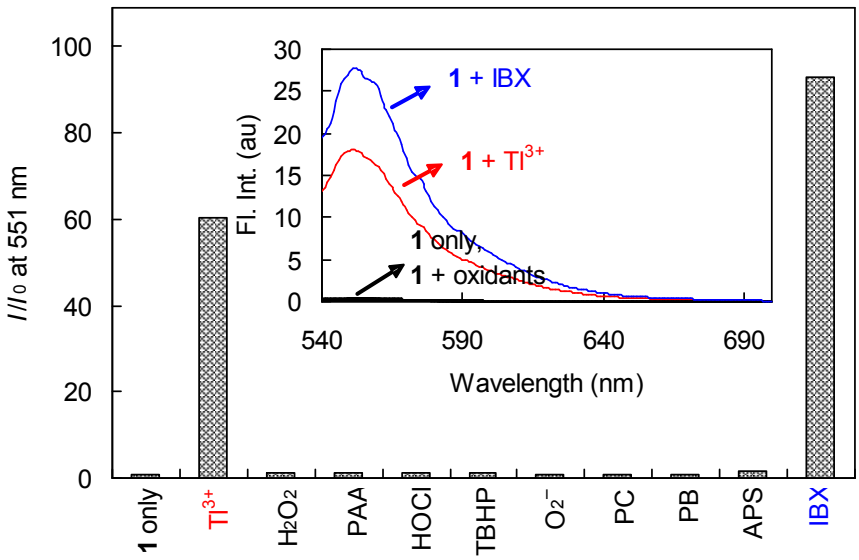

Fig. S10. Changes in fluorescence enhancement (I/I_0) of probe **1** at 551 nm in the presence of Tl^{3+} or common oxidants. Inset: fluorescence spectra of **1** in the presence of oxidants. [**1**] = 5.0×10^{-6} M, [Tl^{3+}] = [oxidant] = 1.5×10^{-3} M in acetate buffer solution (pH 4.2, 10 mM) containing 30% (*v*/*v*) DMSO. λ_{ex} = 527 nm.

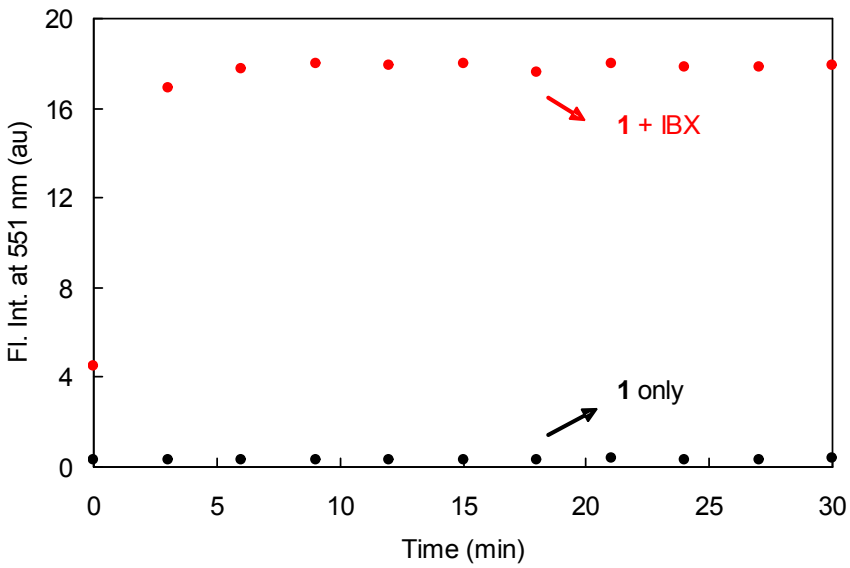

Fig. S11. Time plot of the fluorescence intensity change of IBX signaling by probe **1** at 551 nm. [**1**] = 5.0×10^{-6} M, [IBX] = 1.5×10^{-3} M in acetate buffer solution (pH 4.2, 10 mM) containing 30% (*v*/*v*) DMSO. λ_{ex} = 527 nm.

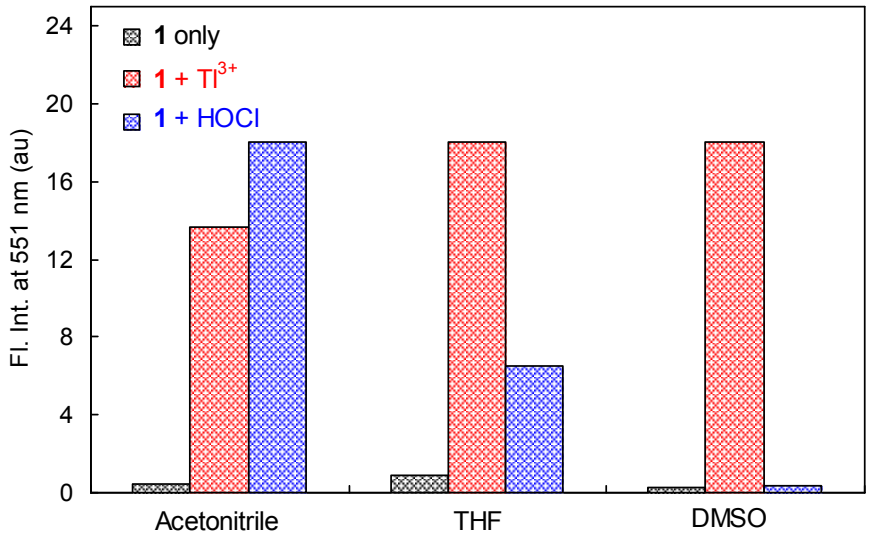

Fig. S12. Effect of solvents on the fluorescence signaling of probe **1** in the presence of Tl^{3+} and HOCl. [**1**] = 5.0 × 10^{-6} M, [Tl^{3+}] = 1.5 × 10^{-3} M, [HOCl] = 5.0 × 10^{-5} M in a solution of acetate buffer (pH 4.2, 10 mM) comprising 30% (*v*/*v*) acetonitrile, THF or DMSO. λ_{ex} = 527 nm.

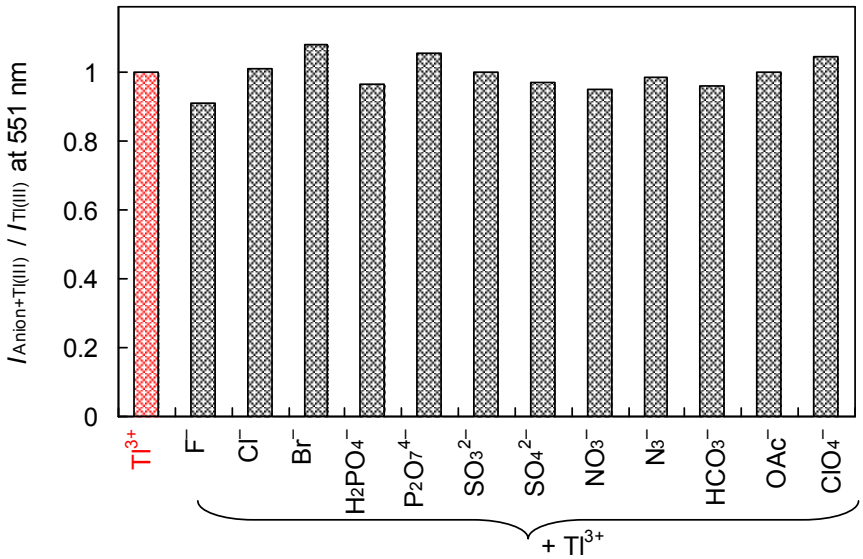

Fig. S13. Changes in fluorescence intensity ratio ($I_{Anion+Tl(III)}/I_{Tl(III)}$) of Tl^{3+} signaling by probe **1** at 551 nm under the competitive conditions of the presence of common anions. [**1**] = 5.0 × 10^{-6} M, [Tl^{3+}] = [A^{n-}] = 1.5 × 10^{-3} M in acetate buffer solution (pH 4.2, 10 mM) containing 30% (*v*/*v*) DMSO. λ_{ex} = 527 nm.

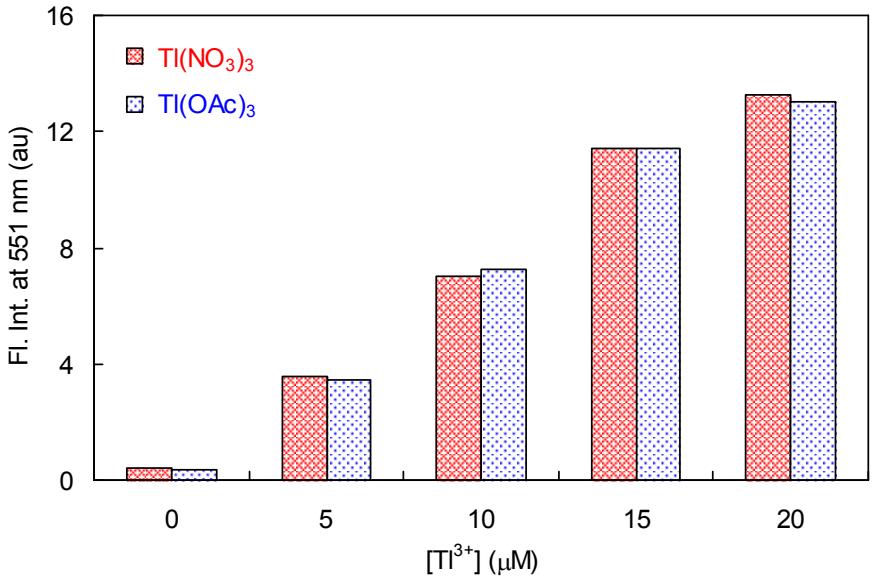

Fig. S14. Tl^{3+} signaling behavior of probe **1** as a function of $Tl(NO_3)_3$ and $Tl(OAc)_3$ concentration. [**1**] = 5.0×10^{-6} M, $[Tl(NO_3)_3] = [Tl(OAc)_3] = 0 – 2.0 \times 10^{-5}$ M in a solution of acetate buffer (pH 4.2, 10 mM) containing 30% (*v/v*) DMSO. λ_{ex} = 527 nm.

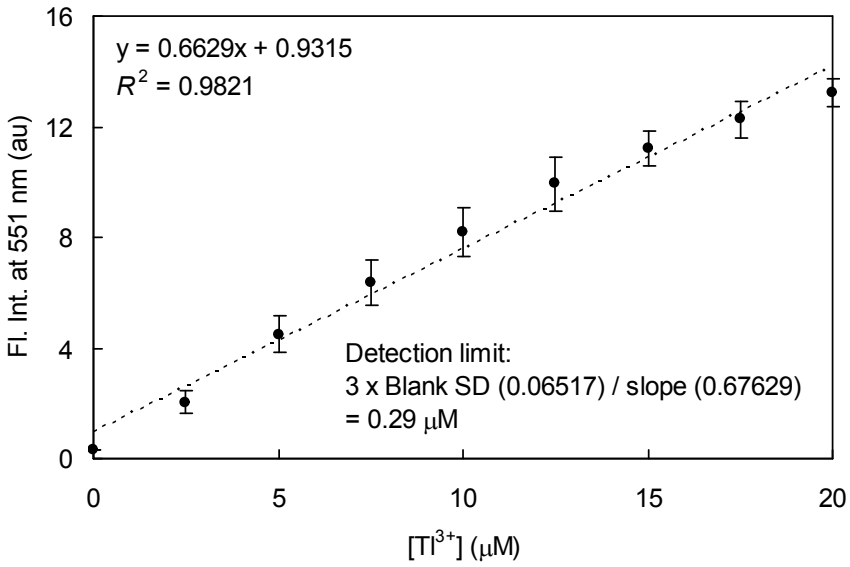

Fig. S15. Tl^{3+} concentration-dependent fluorescence changes of probe **1** at 551 nm. [**1**] = 5.0×10^{-6} M, $[Tl^{3+}] = 0 – 2.0 \times 10^{-5}$ M in acetate buffer solution (pH 4.2, 10 mM) containing 30% (*v/v*) DMSO. λ_{ex} = 527 nm.

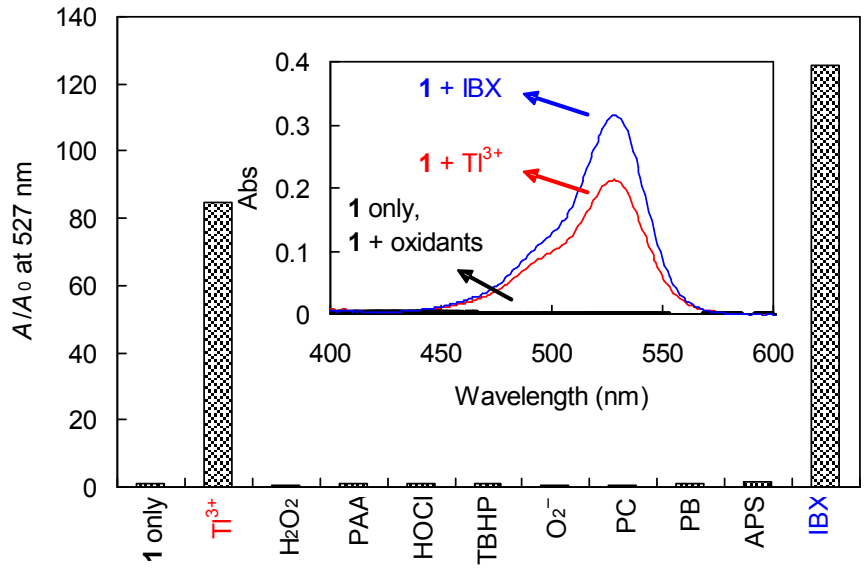

Fig. S16. Changes in absorbance enhancement (A/A_0) of probe **1** at 527 nm in the presence of common oxidants. Inset: absorption spectra of **1** in the presence of oxidants. [**1**] = 5.0×10^{-6} M, [oxidant] = 1.5×10^{-3} M in acetate buffer solution (pH 4.2, 10 mM) containing 30% (*v/v*) DMSO.

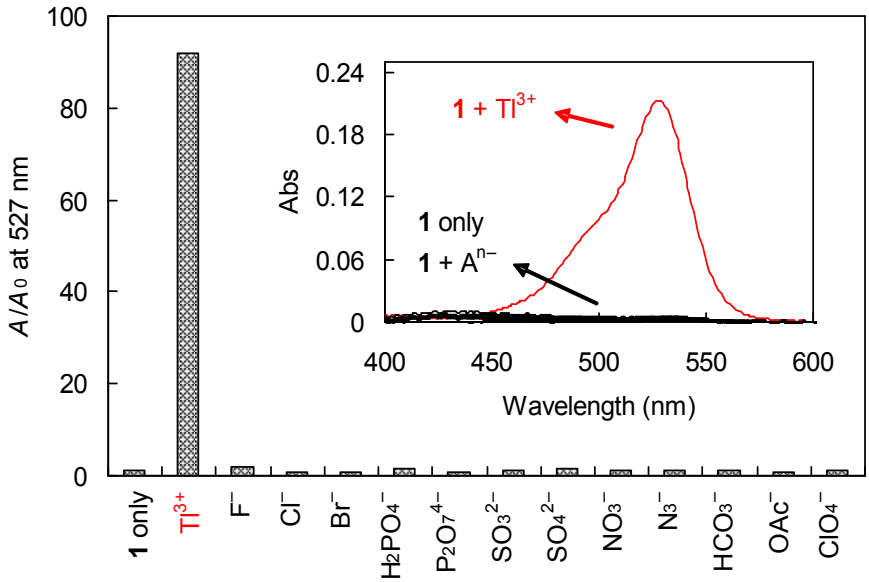

Fig. S17. Changes in absorbance enhancement (A/A_0) of probe **1** at 527 nm in the presence of common anions. Inset: absorption spectra of **1** in the presence of anions. [**1**] = 5.0×10^{-6} M, [A^{n-}] = 1.5×10^{-3} M in acetate buffer solution (pH 4.2, 10 mM) containing 30% (*v/v*) DMSO.

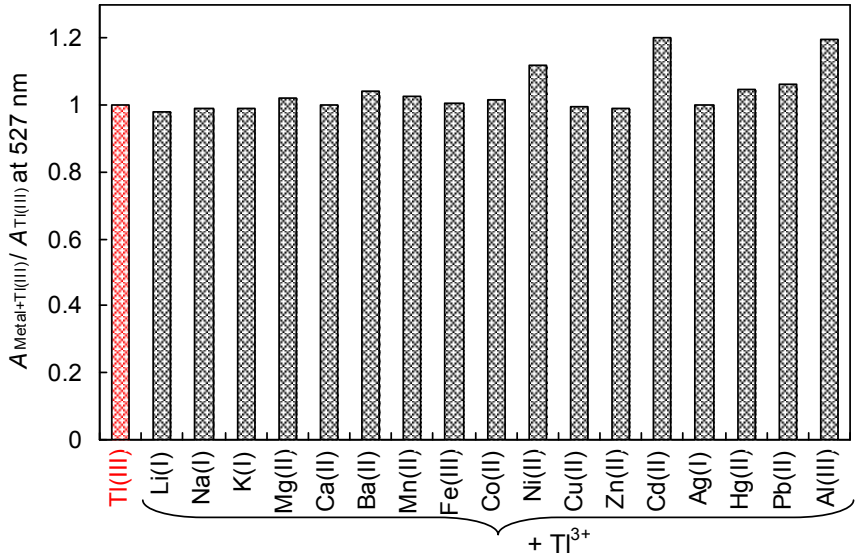

Fig. S18. Changes in absorbance enhancement (A/A_0) of Tl^{3+} signaling by probe **1** at 527 nm under the competitive conditions of the presence of common metal ions. [**1**] = 5.0×10^{-6} M, $[Tl^{3+}] = [M^{n+}] = 1.5 \times 10^{-3}$ M in acetate buffer solution (pH 4.2, 10 mM) containing 30% (*v/v*) DMSO.

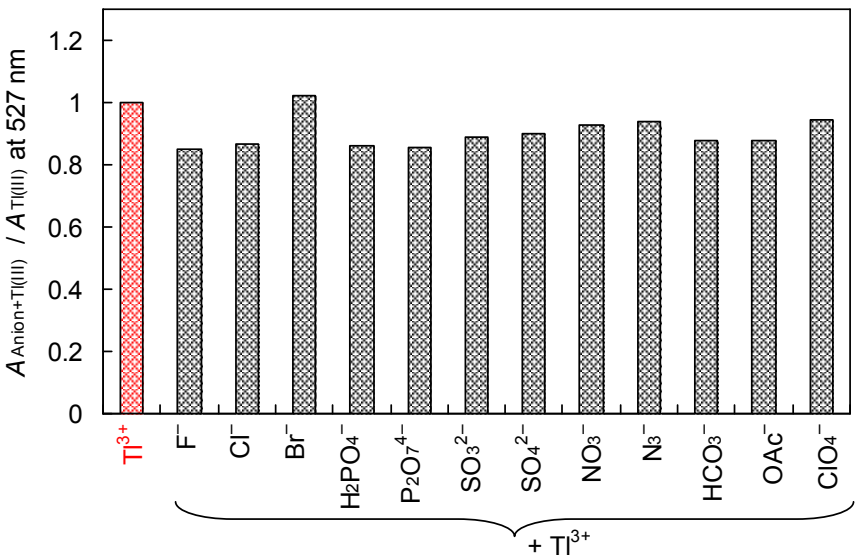

Fig. S19. Changes in absorbance enhancement (A/A_0) of Tl^{3+} signaling by probe **1** at 527 nm under the competitive conditions of the presence of common anions. [**1**] = 5.0×10^{-6} M, $[Tl^{3+}] = [A^{n-}] = 1.5 \times 10^{-3}$ M in acetate buffer solution (pH 4.2, 10 mM) containing 30% (*v/v*) DMSO.

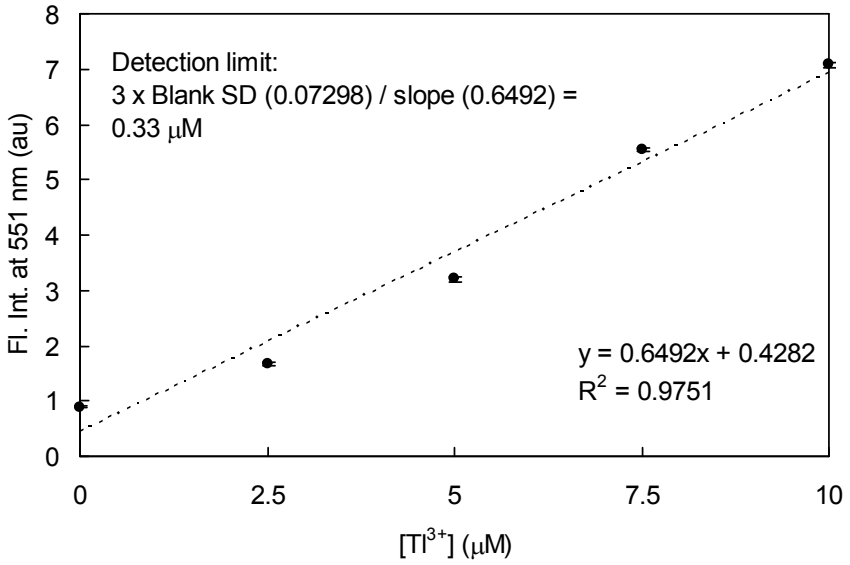

Fig. S20. Changes in the fluorescence intensity at 551 nm of probe **1** as a function of concentration of thallium ions in a synthetic urine. [**1**] = 5.0×10^{-6} M, $[Tl^{3+}]$ = 0 – 10 μM in acetate buffer solution (pH 4.2, 10 mM) consisting 30% (*v/v*) DMSO. λ_{ex} = 527 nm.

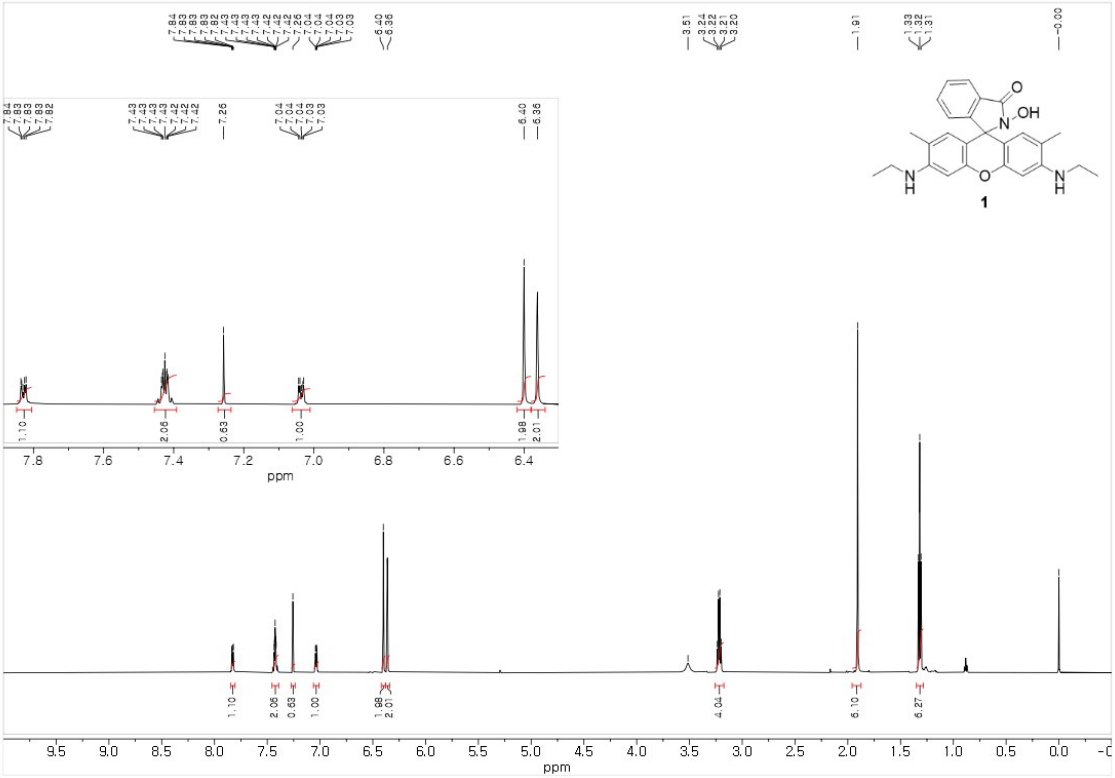

Fig. S21. ^{1}H NMR spectrum of **1** in $CDCl_3$.

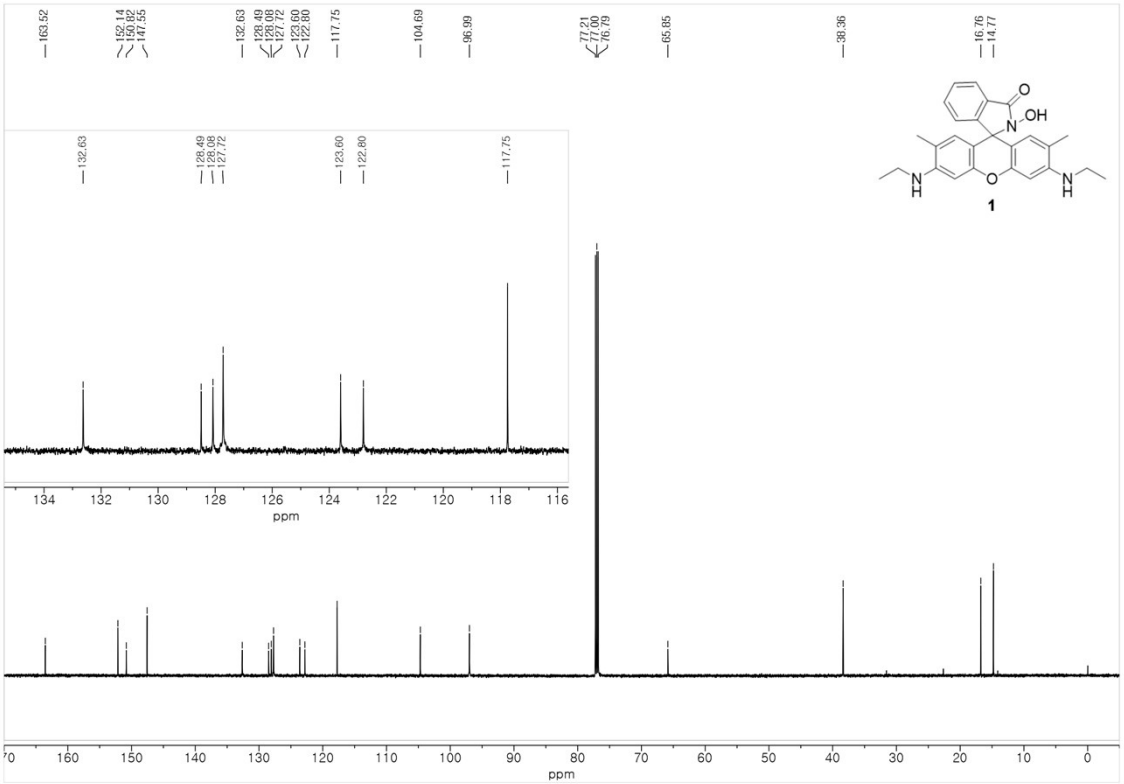

Fig. S22. ^{13}C NMR spectrum of **1** in $CDCl_3$.

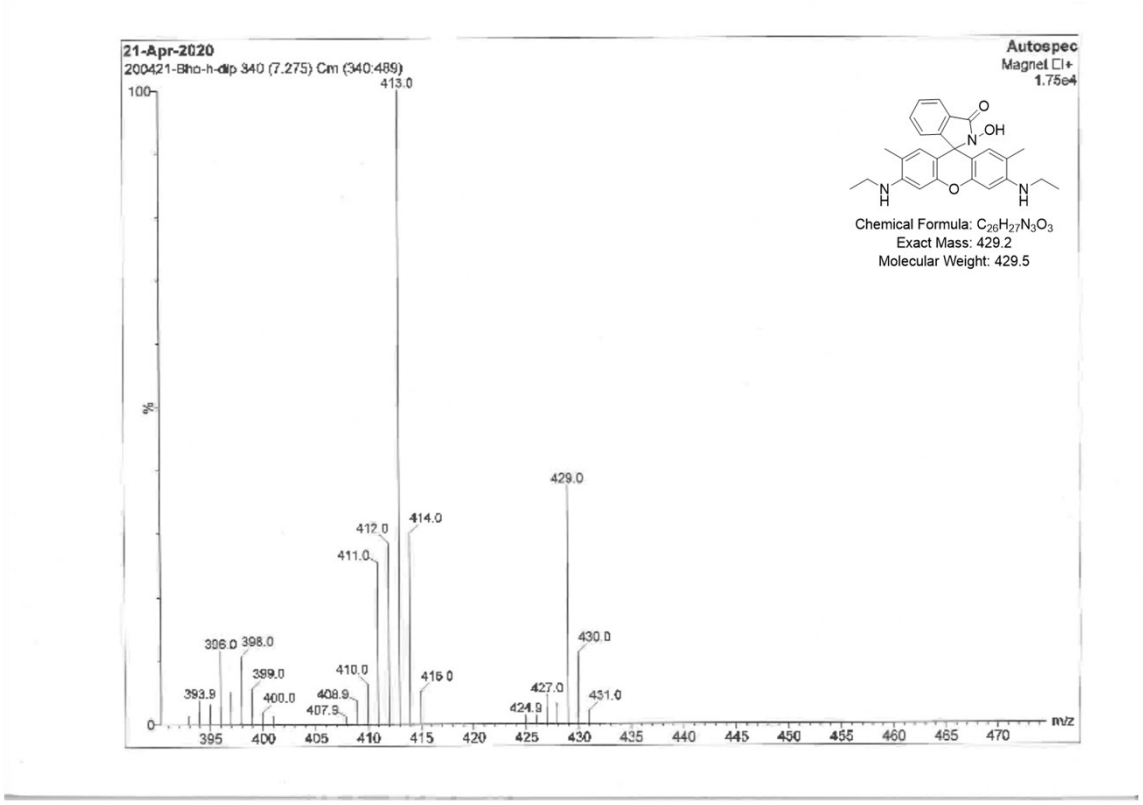

Fig. S23. EI (direct insertion probe) mass spectrum of **1**.

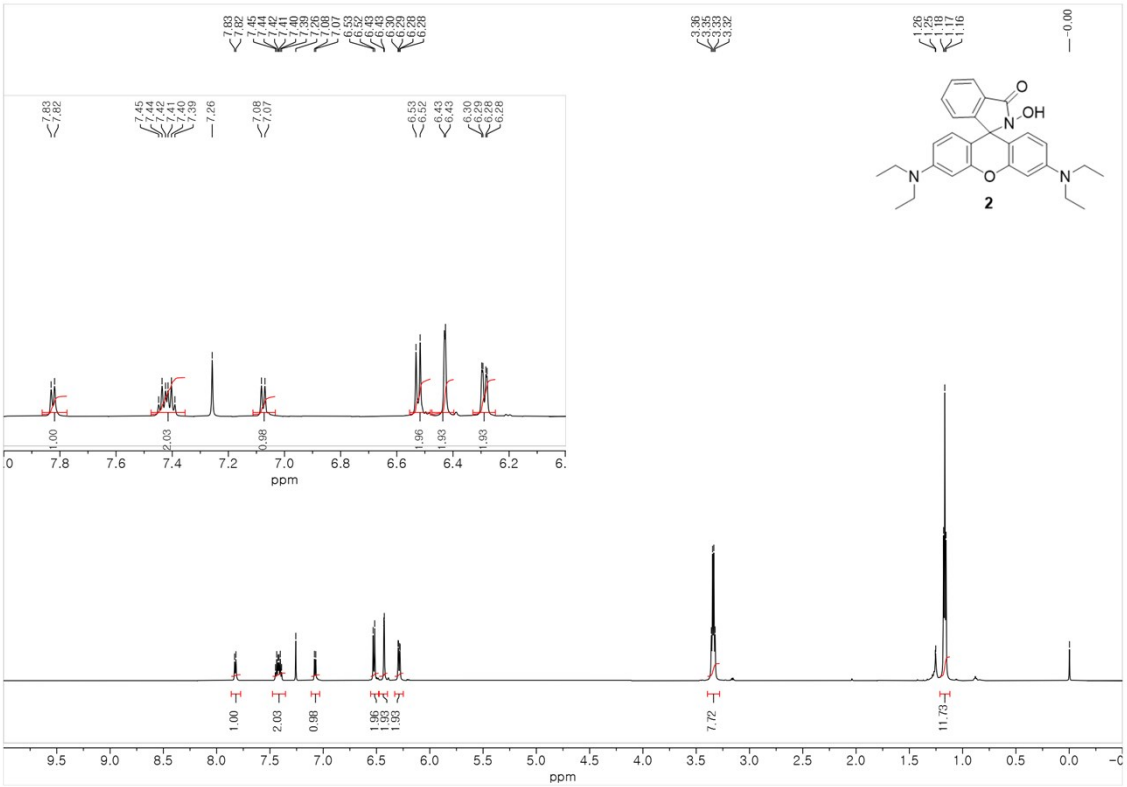

Fig. S24. ^{1}H NMR spectrum of **2** in $CDCl_3$.

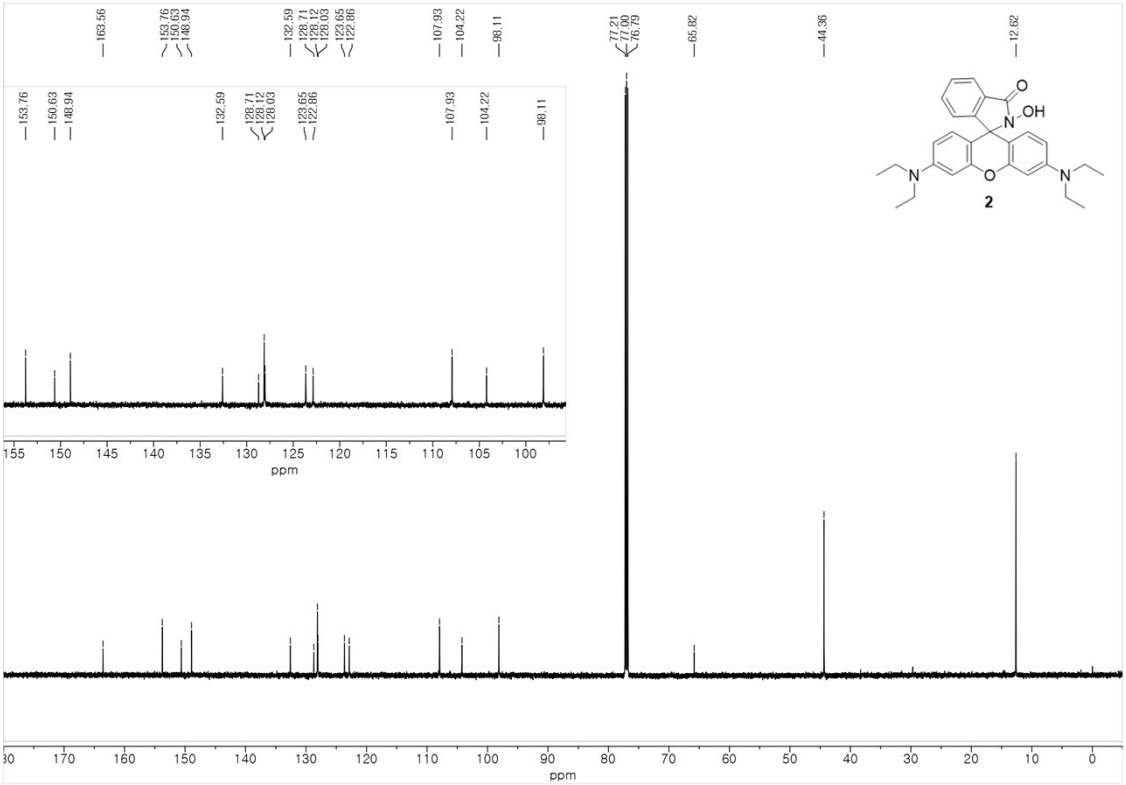

Fig. S25. ^{13}C NMR spectrum of **2** in $CDCl_3$.

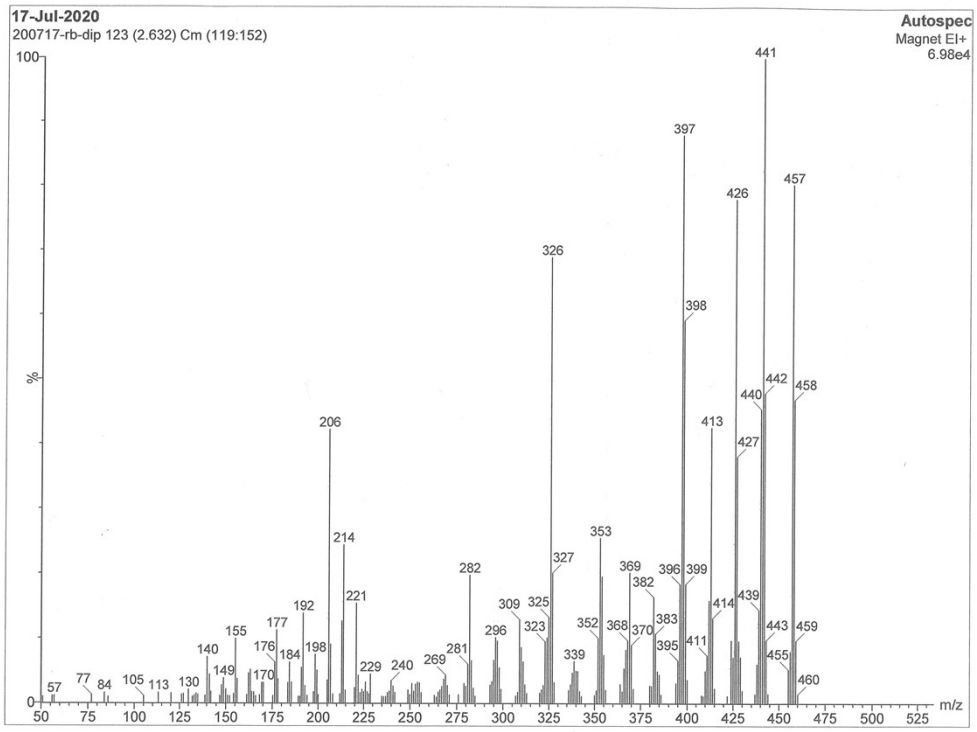

Fig. S26. EI (direct insertion probe) mass spectrum of **2**.

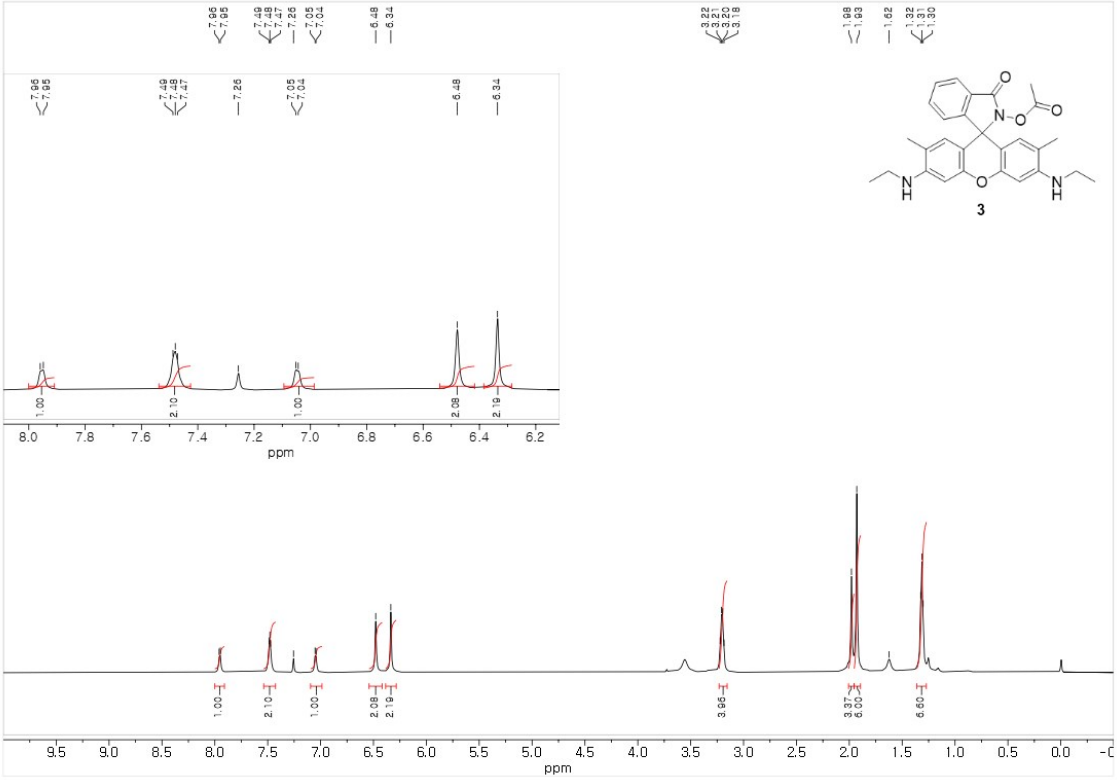

Fig. S27. ^{1}H NMR spectrum of **3** in $CDCl_3$.

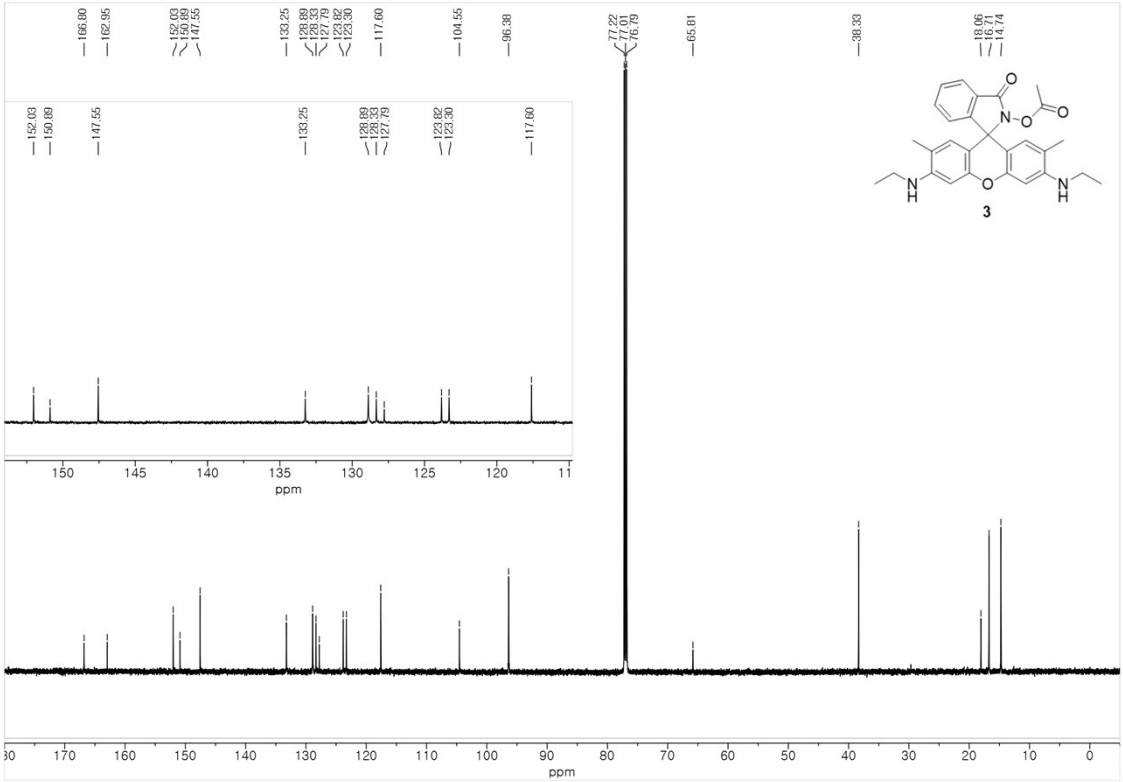

Fig. S28. ^{13}C NMR spectrum of **3** in $CDCl_3$.

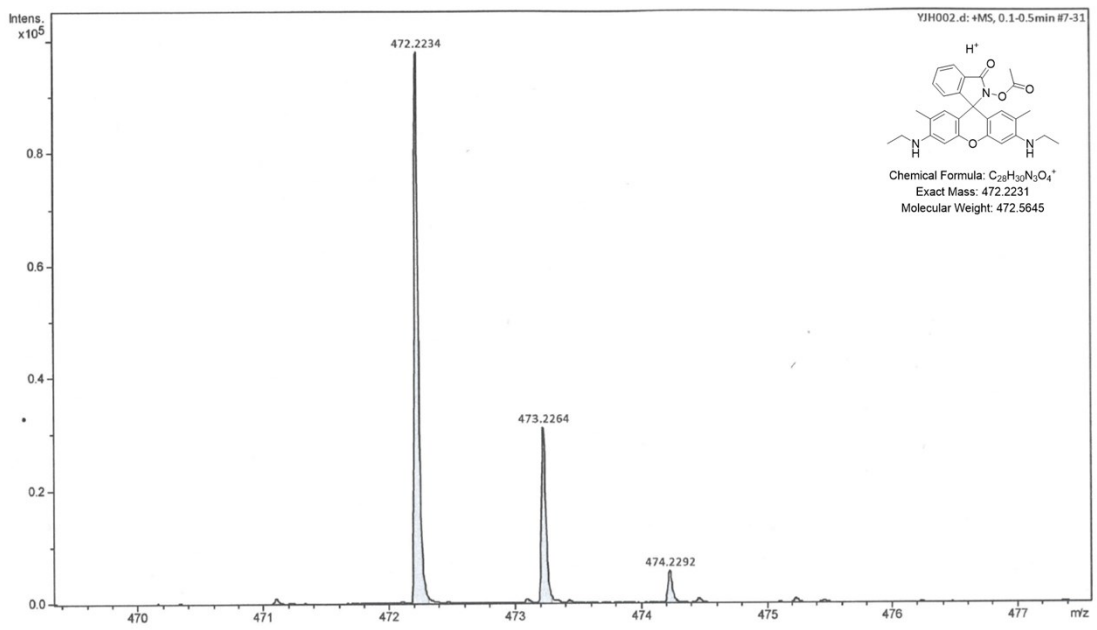

Fig. S29. High resolution ESI mass spectrum of **3**.